The mechanism of Cl incorporation in amphibole

Roberta Oberti, Luciano Ungaretti, Elio Cannillo, Frank C. Hawthorne*

Centro di Studio per la Cristallochimica e la Cristallografia, via Bassi 4, I-27100 Pavia, Italy

Abstract

The crystal structure of three calcic $C2/m$ amphiboles with different Cl contents have been refined to R indices of ~2% using MoKα X-radiation. The monovalent anion site is split into two distinct sites, O3 and O3′ that are separated by ~0.5 Å along [100] and are occupied by (OH,F) and Cl, respectively. The variation in bond lengths to the O3 and O3′ sites as a function of cation and anion site populations can be interpreted in terms of a strong preference for Fe^{2+}-Cl short-range order. Bond-strength arguments and observed interatomic distances indicate a significant bonding interaction between K at the A site and Cl at the O3′ site. The expansion of the octahedral sheet caused by the incorporation of Cl requires a concomitant expansion of the tetrahedral chain that occurs partly by chain straightening but primarily by the increased substitution of $^{[4]}Al$ for Si. The details of the incorporation mechanism indicate that increasing Cl content in amphiboles requires increasing Fe^{2+}, K, and $^{[4]}Al$; compositional correlations of this sort are observed in Cl-bearing amphiboles.

Introduction

Fluids are an important feature of most geochemical processes. They control the dissolution, transport, crystallization, and alteration of minerals, and their character has a major effect on the stability and composition of their coexisting minerals. Halogens are particularly important fluid components in many environments, as they can greatly affect the stabilities of minerals with monovalent anion components (OH^-, F^-, Cl^-) and can greatly enhance the solubility and transport of specific metals by means of complexation in the fluid phase. As the fluid is normally a fugitive phase, we rely on the compositions of halogen-OH-bearing phases to give an indication of the fugacity of the halogen species present in the original fluid. In the ideal case, such minerals would have constant composition, exerting no compositionally variable constraints on halogen-OH incorporation. Unfortunately, this is not the case, and most work has involved micas, amphiboles, and apatite, all of which show extensive compositional effects.

Until recently, Cl tended to be ignored as a significant component of amphiboles and was only reported as an oddity (Krutov, 1936; Dick and Robinson, 1979; Kaminemi et al., 1982; Gulyaeva et al., 1986; Suwa et al., 1987) despite its documented importance in common geological environments (Buddington and Leonard, 1953; Borley, 1962; Leelanandam, 1970). More recent work (Ito and Anderson, 1983; Mevel, 1984; Volfinger et al., 1985; Vanko, 1986; Castelli, 1988; Morrison, 1991; Enami et al., 1993) has shown that Cl contents of amphiboles from associated parageneses can vary widely, and there are in-dications of complex crystal-chemical constraints exerted by the amphibole structure on the incorporation of Cl at the O3 site. However, several sometimes conflicting relationships have been proposed between amphibole composition and Cl content. Here we examine the structural aspects of Cl substitution in amphiboles and attempt to resolve the principal compositional constraints on Cl incorporation.

Experimental

The Cl-bearing crystals used in this work are from the Sesia-Lanzo marbles, Western Italian Alps [Castelli, 1988, AN-2 and AN-4 corresponding to samples Cl(1) and Cl(2) of this study]; their crystal-chemical behavior was compared with that of a Cl-free amphibole of similar composition from a contact-metamorphosed pelitic carbonate found in the Nuptse Glacier moraine, Everest Massif, Nepal [sample Cl(0)]. All samples crystallized around 500 °C.

X-ray data measurement

Crystals were selected for unit-cell and intensity measurements on the basis of optical clarity, freedom from inclusions, and equant shape. All crystals were mounted on a Philips PW 1100 automated four-circle diffractometer and studied with graphite-monochromated MoKα X-radiation; crystal quality was assessed by means of the profiles and widths of Bragg diffraction peaks. Unit-cell dimensions were calculated from least-squares refinement of the d values obtained for 48 rows of the reciprocal lattice by measuring the center of gravity of each reflection and of its corresponding antireflection in the θ range between -30 and $+30°$; values for the crystals used in the measurement of the intensity data are given in Table 1.

* Permanent address: Department of Geological Sciences, University of Manitoba, Winnipeg, Manitoba R3T 2N2, Canada.

TABLE 1. Selected structure refinement data

	Cl(0)	Cl(1)	Cl(2)
a (Å)	9.895(1)	9.884(1)	9.922(1)
b (Å)	18.119(1)	18.143(5)	18.219(1)
c (Å)	5.332(1)	5.332(1)	5.360(1)
β (°)	105.17(1)	104.86(1)	104.81(1)
V (Å³)	922.6	924.2	936.7
θ_{max} (°)	30	40	40
Space group	$C2/m$	$C2/m$	$C2/m$
Number*	289	399	398
No. of $|F|$	1287	1506	1540
No. of $|F_o|$	1269	987	991
R_{sym} (%)	2.1	2.3	2.5
R_{obs} (%)	1.4	2.3	1.8
R_{all} (%)	1.5	4.2	4.1

* Number in the amphibole data bank at Pavia.

Intensity data were measured for the monoclinic equivalent pairs hkl and $h\bar{k}l$ in the Laue group $2/m$ using the step-scan profile technique of Lehman and Larsen (1974). Full details of the data measurement procedure are given in Ungaretti (1980) and Ungaretti et al. (1981). The intensity data were corrected for absorption by the method of North et al. (1968), corrected for Lorentz and polarization effects, averaged, and reduced to structure factors. A reflection is considered as observed if its intensity exceeds that of 5 sd, based on counting statistics.

Structure refinement

Fully ionized scattering factors were used for nontetrahedral cations, whereas scattering factors for both neutral and ionized atoms were used for the tetrahedral cations and the O atoms (Ungaretti et al., 1983).

All the refinements with no weighting were done in space group $C2/m$ and converged to R indices of ~2% (Table 1) for observed reflections. As repeatedly observed in the course of the crystal-chemical study of a very large number of amphiboles (see also Ungaretti, 1980, p. 44–46), full-matrix refinement of scale factor, secondary extinction coefficient, atomic positions, site occupancies, and anisotropic displacement parameters can be carried out without any problem of correlations between the variable parameters; the final results are independent of the scheme used in varying the parameters to be refined. Details of the O3 site refinement are discussed in a later section. Atomic coordinates and equivalent isotropic displacement parameters are given in Table 2, selected interatomic distances are given in Table 3, site-scattering results are given in Table 4, and observed and calculated structure factors are listed in Table 5.[1]

Electron microprobe analysis

The crystals used in the measurement of the intensity data were subsequently analyzed by electron microprobe

[1] A copy of Table 5 may be ordered as Document AM-93-531 from the Business Office, Mineralogical Society of America, 1130 Seventeenth Street NW, Suite 330, Washington, DC 20036, U.S.A. Please remit $5.00 in advance for the microfiche.

TABLE 2. Atomic coordinates and equivalent isotropic displacement factors (Å²)

		Cl(0)	Cl(1)	Cl(2)
O1	x	0.1051(1)	0.1062(1)	0.1039(1)
	y	0.0911(1)	0.0903(1)	0.0915(1)
	z	0.2141(2)	0.2139(3)	0.2131(3)
	B_{eq}	0.79	0.89	0.86
O2	x	0.1199(1)	0.1210(2)	0.1215(1)
	y	0.1756(1)	0.1754(1)	0.1777(1)
	z	0.7358(2)	0.7343(3)	0.7365(3)
	B_{eq}	0.70	0.84	0.80
O3	x	0.1097(2)	0.1061(2)	0.1031(2)
	y	0	0	0
	z	0.7120(4)	0.7076(3)	0.7021(3)
	B_{eq}	0.84	1.03	0.93
O3′	x	—	0.1596(3)	0.1611(3)
	y	—	0	0
	z	—	0.7332(4)	0.7337(5)
	B_{eq}	—	1.64	1.22
O4	x	0.3686(1)	0.3679(2)	0.3690(1)
	y	0.2499(0)	0.2495(1)	0.2499(1)
	z	0.7924(2)	0.7944(3)	0.7947(3)
	B_{eq}	0.82	0.90	0.92
O5	x	0.3490(1)	0.3484(2)	0.3474(1)
	y	0.1392(0)	0.1363(1)	0.1363(1)
	z	0.1087(2)	0.1007(3)	0.0985(3)
	B_{eq}	0.87	0.96	0.89
O6	x	0.3426(1)	0.3426(2)	0.3423(1)
	y	0.1195(0)	0.1201(1)	0.1220(1)
	z	0.6046(3)	0.5978(3)	0.5977(3)
	B_{eq}	0.91	1.02	1.01
O7	x	0.3336(2)	0.3359(3)	0.3338(2)
	y	0	0	0
	z	0.2887(4)	0.2911(5)	0.2977(4)
	B_{eq}	1.21	1.22	1.33
T1	x	0.2791(1)	0.2789(1)	0.2779(1)
	y	0.0860(1)	0.0854(1)	0.0861(1)
	z	0.3026(1)	0.2996(1)	0.3006(1)
	B_{eq}	0.45	0.52	0.49
T2	x	0.2911(1)	0.2909(1)	0.2911(1)
	y	0.1732(1)	0.1729(1)	0.1735(1)
	z	0.8140(1)	0.8100(1)	0.8113(1)
	B_{eq}	0.46	0.53	0.54
M1	x	0	0	0
	y	0.0897(1)	0.0921(1)	0.0944(1)
	z	½	½	½
	B_{eq}	0.58	0.69	0.73
M2	x	0	0	0
	y	0.1780(1)	0.1787(1)	0.1792(1)
	z	0	0	0
	B_{eq}	0.50	0.60	0.59
M3	x	0	0	0
	y	0	0	0
	z	0	0	0
	B_{eq}	0.53	0.73	0.71
M4	x	0	0	0
	y	0.2808(1)	0.2796(1)	0.2806(1)
	z	½	½	½
	B_{eq}	0.75	0.93	0.85
A	x	0	0	0
	y	½	½	½
	z	0	0	0
	B_{eq}	2.20	4.58	2.75
Am	x	0.0336(6)	0.0412(6)	0.0344(4)
	y	½	½	½
	z	0.0734(8)	0.0945(8)	0.0707(7)
	B_{eq}	1.74	4.66	3.38
A2	x	0	0	0
	y	0.4714(6)	0.4614(6)	0.4645(6)
	z	0	0	0
	B_{eq}	4.05	3.00	4.72
H	x	0.1579(2)	—	—
	y	0	—	—
	z	0.7603(2)	—	—
	B_{eq}	1.53	—	—

TABLE 3. Selected interatomic distances (Å) and angles (°)*

	Cl(0)	Cl(1)	Cl(2)
T1-O1	1.665	1.652	1.672
T1-O5	1.688	1.680	1.694
T1-O6	1.681	1.676	1.689
T1-O7	1.657	1.654	1.665
⟨T1-O⟩	1.672	1.666	1.680
T2-O2	1.636	1.625	1.629
T2-O4	1.606	1.598	1.606
T2-O5	1.645	1.648	1.643
T2-O6	1.658	1.660	1.656
⟨T2-O⟩	1.636	1.632	1.633
M1-O1 × 2	2.058	2.062	2.060
M1-O2 × 2	2.152	2.124	2.140
M1-O3 × 2	2.110	2.126	2.147
M1-O3′ × 2	—	2.412	2.462
⟨M1-O,O3⟩	2.107	2.104	2.116
⟨M1-O,O3′⟩	—	2.199	2.221
M2-O1 × 2	2.060	2.088	2.078
M2-O2 × 2	2.066	2.076	2.078
M2-O4 × 2	1.967	1.967	1.959
⟨M2-O⟩	2.031	2.043	2.039
M3-O1 × 4	2.119	2.115	2.132
M3-O3 × 2	2.100	2.091	2.105
M3-O3′ × 2	—	2.380	2.400
⟨M3-O,O3⟩	2.112	2.107	2.123
⟨M3-O,O3′⟩	—	2.203	2.221
M4-O2 × 2	2.417	2.408	2.408
M4-O4 × 2	2.343	2.345	2.355
M4-O5 × 2	2.657	2.732	2.747
M4-O6 × 2	2.541	2.533	2.508
⟨M4-O⟩	2.489	2.505	2.504
A-O5 × 4	3.063	3.010	3.025
A-O6 × 4	3.137	3.171	3.212
A-O7 × 2	2.531	2.516	2.571
⟨A-O⟩	2.986	2.976	3.009
Am-O5 × 2	3.148	3.127	3.127
Am-O5 × 2	3.040	2.995	2.985
Am-O6 × 2	2.835	2.791	2.913
Am-O7	2.534	2.511	2.585
Am-O7	3.310	3.189	3.302
Am-O7	2.605	2.642	2.632
⟨Am-O⟩	2.944	2.907	2.952
A2-O5 × 2	2.652	2.467	2.521
A2-O6 × 2	2.804	2.737	2.803
A2-O7 × 2	2.584	2.611	2.651
⟨A2-O⟩	2.680	2.605	2.658
M1-M1	3.249	3.341	3.440
M1-M2	3.110	3.095	3.093
M1-M3	3.122	3.146	3.184
M1-M4	3.463	3.403	3.393
M2-M3	3.225	3.242	3.264
M2-M4	3.252	3.234	3.256
O5-O6-O5	164.5	167.1	168.7
T1-O5-T2	134.7	135.9	136.5
T1-O6-T2	138.9	139.1	139.7
T1-O7-T1	140.3	139.0	140.8
O3-O3′	—	0.51	0.56
A-O3	3.764	3.804	3.853
A-O3′	—	3.300	3.300
Am-O3	3.414	3.373	3.490
Am-O3′	—	2.863	2.933
A2-O3	3.800	3.868	3.907
A2-O3′	—	3.373	3.363

* Standard deviations are ≤1 in the last digit.

TABLE 4. Refined site-scattering values (electrons) compared with numbers of electrons calculated from normalized formulae (EMP)

	Cl(0)	Cl(1)	Cl(2)
M1	39.2	42.1	47.0
M2	39.3	37.2	38.6
M3	21.2	22.4	24.9
Σ (M1, M2, M3)	99.7	101.7	110.5
EMP (M1, M2, M3)	100.4	102.1	109.5
M4	39.4	38.7	38.8
EMP M4	39.5	38.6	38.6
A	9.6	13.2	15.4
EMP A	10.6	11.8	14.1
Σ (O3, O3′)	16.0	21.5	25.2
EMP O3	16.3	21.3	25.0

wavelength-dispersive mode. Details of experimental conditions and standard settings are given in Oberti et al. (1992). Each grain was analyzed at a minimum of 12 points to check for compositional zoning and to obtain a representative composition for the whole crystal used in the measurement of diffraction intensities. Data reduction was done with the $\phi(\rho Z)$ method (Pouchou and Pichoir, 1984, 1985).

The formula unit was calculated from the electron microprobe analyses on the basis of 24 (O, OH, F, Cl) assuming O3 = OH + F + Cl, with OH derived by calculation from this constraint. Fe_2O_3 contents were calculated from a relationship between mean bond length and the constituent cation radius for the M2 site, combined with the results of site-scattering refinement. Final formulae are given in Table 6.

SITE POPULATIONS

The site-scattering results (Table 4) are given in terms of the total number of electrons per formula unit of the atoms at each site; in order to derive site populations, these must be assigned to specific cations and anions. From these results, we may calculate the numbers of electrons at the sites corresponding to the A-, B-, and C-group cations; we may also calculate these values from the formula unit derived from the electron microprobe results. The measure of agreement between these two sets of results (Table 4) is a check on both the crystal structure refinement and the electron microprobe analyses. For the B- and C-group cations, the agreement is extremely good, being 0.1 and 0.7 electrons (e), respectively. The agreement for the A-group cations is less satisfactory, being 1.2 e. The site populations were then obtained by taking into account all information from the EMP analyses and the structure refinements.

T1 and T2 sites

The ⟨T1-O⟩ and ⟨T2-O⟩ distances indicate significant [4]Al ordered at the T1 site. The various predictive curves for [4]Al based on ⟨T-O⟩ bond lengths (Hawthorne, 1983; Ungaretti and Oberti, unpublished manuscript) give good agreement for samples Cl(0) and Cl(1) but slightly overestimate the [4]Al at high Cl [crystal Cl(2)].

(EMP) techniques. The crystals were mounted in piccolite in small holes in a 1-in. perspex disk containing a crystal of tremolite (specimen 56 of Hawthorne, 1983) to check for analytical accuracy.

Electron microprobe analysis was done on a fully automated Cameca SX-50 instrument operating in the

TABLE 6. Average electron microprobe analyses (wt%) and unit formulae

	Cl(0)	Cl(1)	Cl(2)
SiO_2	38.95	41.22	38.24
Al_2O_3	12.35	10.71	11.81
TiO_2	0.56	0.24	0.16
Fe_2O_3*	6.61	3.39	5.76
FeO	15.09	19.67	20.17
MnO	0.59	0.26	0.24
MgO	7.47	6.66	4.31
CaO	11.51	10.34	10.64
Na_2O	1.17	2.16	1.64
K_2O	1.94	1.77	2.60
F	0.55	0.54	0.27
Cl	0.00	2.12	3.60
H_2O**	(1.65)	(1.12)	(0.81)
O = F, Cl	−0.23	−0.58	−0.75
Total	98.25	99.63	99.50
Si	6.094	6.473	6.185
Al	1.906	1.527	1.815
Σ T	8.000	8.000	8.000
Al	0.372	0.456	0.437
Ti	0.066	0.028	0.020
Fe^{3+}	0.778	0.401	0.701
Fe^{2+}	1.975	2.583	2.729
Mn^{2+}	0.078	0.035	0.033
Mg	1.742	1.559	1.039
Σ C	5.012	5.062	4.958
Δ	0.012	0.062	—
Ca	1.930	1.740	1.844
Na	0.058	0.198	0.156
Σ B	2.000	2.000	2.000
Na	0.297	0.460	0.358
K	0.387	0.355	0.537
Σ A	0.684	0.815	0.895
F	0.27	0.27	0.14
Cl	—	0.56	0.98
(OH)	1.73	1.17	0.88
Σ O3	2.00	2.00	2.00

Note: Atoms per formula unit.
* Fe^{3+}/Fe^{2+} ratio derived from structure refinement results.
** Calculated assuming (OH + F + Cl) = 2 apfu.

TABLE 7. Site populations

		Cl(0)	Cl(1)	Cl(2)
T1	Si	2.09	2.44	2.15
	Al	1.91	1.56	1.85
T2	Si	4.00	4.00	4.00
M1	Mg	0.91	0.71	0.36
	Fe^{2+}	1.09	1.29	1.64
M2	Mg	0.54	0.76	0.62
	Fe^{2+}	0.24	0.33	0.30
	Al	0.37	0.32	0.34
	Fe^{3+}	0.78	0.56	0.72
	Ti^{4+}	0.07	0.03	0.02
M3	Mg	0.34	0.26	0.08
	Fe^{2+}	0.66	0.74	0.92
M4	(Mn,Fe)	0.01	0.06	—
	Ca	1.93	1.74	1.85
	Na	0.06	0.20	0.15
A	Na	0.30	0.46	0.36
	K	0.38	0.36	0.54
O3	Cl	0.00	0.56	0.98
	F	0.27	0.27	0.14
	OH*	1.73	1.17	0.88

* Calculated assuming complete monovalent anion occupancy at O3.

ther details). The resultant M2 site populations are given in Table 7. Note that the [6]Al values in the formula unit from EMP analyses (Table 6) and the M2 site populations (Table 7) are independent estimates; their good agreement indicates the accuracy of both sets of measurements and of the Fe^{3+}/Fe^{2+} ratios.

The M4 and A sites

The M4 site shows negligible occupancy of small divalent cations (Table 7) but small amounts of Na are present, as indicated by both the formula unit (Table 6) and the refined site-scattering (Table 4). In all cases, the A site is more than half-occupied, with approximately equal amounts of Na and K.

The O3 site

The electron microprobe analyses show the O3 site to have small amounts of F⁻, the principal variations across the series involving Cl⁻ and OH⁻ (Table 6). The effects of the Cl⁻ ⇌ OH⁻ substitution are shown in Figure 1 by a series of Fourier maps through the O3 site in the (010) plane. In sample Cl(0), with Cl = 0.0 apfu, the O3 density is fairly isotropic, showing only a slight elongation, approximately along [100], that is due to the presence of major (O) and minor (H) scatterers ~1 Å apart in this direction. With increasing Cl, the O3 density becomes much more anisotropic, showing a strong elongation subparallel to [100]. In sample Cl(1) (Fig. 1b), the principal center of density is still close to the O3 = OH⁻ position, with a weaker lobe extending away from the normal O3 position and also away from the coordinating M1 and M3 cation positions (not shown). In sample Cl(2) (Fig. 1c), with the maximum amount of Cl, the elongation of the density is more uniform, with the center of maximum density displaced away from the normal O3 position and a slightly weaker lobe extending toward the normal O3 position.

The M1 and M3 sites

These sites are occupied by Mg and Fe^{2+} (plus minor amounts of Mn^{2+}, which we will include with the Fe^{2+}, as they have very similar scattering powers for X-rays). The constraint that these sites be completely occupied allows us to derive the Mg and Fe^{2+} site populations directly from the refined site scattering powers of Table 4; the resultant values are given in Table 7.

The M2 site

The [6]Ti^{4+} content is very low in these crystals and is very unlikely to be related to the $Ti^{4+} + 2O^{2-} \rightleftharpoons (Mg,Fe^{2+}) + 2OH^-$ substitution (see Oberti et al., 1992); hence [6]Ti^{4+} was assigned to the M2 site. Reliable estimates of the Mg, Al, Fe^{2+}, and Fe^{3+} contents at M2 can be obtained by taking into account the following crystal-chemical constraints: full occupancy of the site, observed scattering powers, ⟨M2-O⟩ distance, overall neutrality of the formula unit. A system of four equations was solved, in which the observed values for these quantities were considered to be a linear combination of the values observed for a single cation occupancy multiplied by the relative unknown populations (see Ungaretti et al., 1981, for fur-
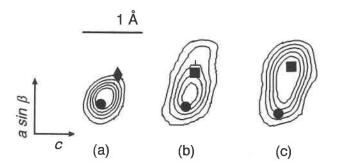
Fig. 1. Fourier maps through the O3 site on (010) in amphiboles: (a) crystal Cl(0), (b) crystal Cl(1), (c) crystal Cl(2). Circles indicate the position of the O atom, squares that of Cl, and the diamond that of H. Contours are drawn at 5, 10, 15, 20, and 25 e/Å³.

We interpret Figure 1 in terms of a split O3 position (O3 and O3′), whereby O3 is occupied by OH⁻ and F⁻, and O3′ is occupied by Cl⁻. In order to get a better idea of the local environments around O3 in each of these cases, the O3 anion was split into two sites, O3 and O3′, that were refined independently; the refined data of Tables 2, 3, and 4 are for this split-site model. There is a significant separation of the two split sites of ~0.5 Å, and this separation is subparallel to [100].

In order to make the following discussion about the structural effects of Cl substitution at O3 clearer, Figure 2 shows the geometrical relationships among O3, O3′, and the other parts of the amphibole structure.

CHEMICAL CORRELATIONS AND PROPOSED MECHANISMS

It has long been known that all Cl-rich amphiboles are potassium hastingsite, rich in K and Fe^{2+} (Krutov, 1936; Dick and Robinson, 1979; Kaminemi et al., 1982). Vanko (1986) showed that Cl-bearing amphiboles were enriched in [4]Al relative to Cl-free amphiboles in metabasites from Mathematician Ridge, East Pacific Ocean. Similar relationships were found by Suwa et al. (1987), Castelli (1988), Morrison (1991), and Enami et al. (1993) for coherent suites of amphiboles. Gulyaeva et al. (1986) and Suwa et al. (1987) showed high Cl values only in Fe-rich amphiboles; Castelli (1988) showed a very well developed correlation between Fe and Cl contents in a suite of amphiboles from the Sesia-Lanzo marbles, from which samples Cl(1) and Cl(2) were taken, and similar correlations were shown by Volfinger et al. (1985) and Enami et al. (1993). Morrison (1991) showed an inverse correlation between Cl and Mg contents of amphiboles. As only Mg and Fe^{2+} occupy the M1 and M3 sites, and the absolute and relative amounts of the small octahedrally coordinated trivalent cations that occupy M2 do not exhibit large variations, then this inverse correlation between Mg and Cl is equivalent to a direct correlation between Fe^{2+} and Cl. Castelli (1988) also showed a strong correlation between Cl and K in a chemically and petrologically similar suite of amphiboles, and Morrison (1991) and Enami
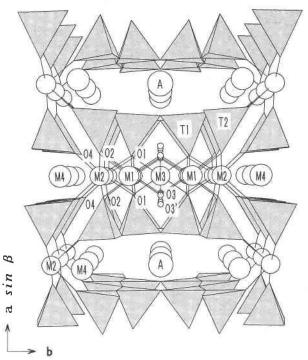

Fig. 2. A projection of the amphibole structure on the (001) plane, showing the steric relationships among O3, O3′, and the other structural sites.

et al. (1993) showed similar but more scattered correlations in amphibole suites of much more disparate composition. Thus the principal correlations established for Cl-bearing amphiboles are increases in Fe^{2+}, K, and [4]Al contents with increasing Cl content.

Volfinger et al. (1985) have proposed a geometrical model for Cl incorporation into micas and amphiboles; here we will discuss only the application to amphiboles. They stated that the substitution of Fe^{2+} (for Mg) in the octahedral sheet enlarges the structure and therefore leaves more room for the incorporation of Cl. The substitution of Fe^{2+} for Mg does enlarge the octahedral strip but enlarges it only in the amount required to incorporate Fe^{2+} instead of Mg; it does not result in any more room for a larger O3 anion than in the Mg-bearing unit. Volfinger et al. (1985) also argued that the tetrahedral chains must straighten to allow more room for the Cl⁻ anion to be incorporated and that this is promoted by the reduction in [4]Al content. It is certainly not established that Cl⁻ requires a larger A cavity, and this argument does not agree with the positive correlation between [4]Al and Cl observed by Vanko (1986), Suwa et al. (1987), Castelli (1988), Morrison (1991), and Enami et al. (1993).

Cl-CATION INTERACTIONS

M1 and M3 sites

The Cl occupying the O3′ site is bonded to two M1 and one M3 cations in the octahedral strip (Fig. 2). As expected for the large Cl⁻ anion, the M1-O3′ and M3-

O3' bonds are greatly elongated (Table 3) relative to the corresponding bonds to O3 in these (and all other) amphiboles: ~2.4 as compared with ~2.1 Å. The M1-O3' and M3-O3' lengths of 2.38–2.46 Å fall in the typical range of Fe^{2+}-Cl distances in inorganic crystals (e.g., 2.38 Å in $FeCl_2 \cdot 4H_2O$, Penfold and Grigor, 1959; 2.39–2.58 Å in erythrosiderite, Bellanca, 1948). However, the high Fe^{2+} contents at the M1 and M3 sites, at least in crystal Cl(2), indicate most M1-O3' and M3-O3' interactions to be Fe^{2+}-Cl bonds, and the observed distances are in accord with that.

From sample Cl(0) to Cl(2), the M1 and M3 sites become more enriched in Fe^{2+}, with a concomitant increase in the mean cation radii at M1 and M3. However, the bonds not involving O3 or O3', namely M1-O1, M1-O2, and M3-O1, do not show any significant increase in length with increasing cation radius. Hence the necessary expansion of bond length as a result of the substitution of Fe^{2+} for Mg^{2+} must occur primarily in the bonds M1-O3, M1-O3', M3-O3, and M3-O3'. This is evident in the increase in M1-O3 and M3-O3 in sample Cl(2) relative to sample Cl(0), as presumably must also occur in the M1-O3' and M3-O3' bonds, although that effect is obscured by the large increase in length caused by the $Cl^- \rightleftharpoons OH^-$ substitution. It is notable that despite a small increase in Fe^{2+} at M3 in sample Cl(1) relative to sample Cl(0) (Table 7), the average value of the M3-O1 and M3-O3 bond lengths decreases slightly; this suggests local ordering of Fe^{2+}-Cl^- and Mg-OH^-.

There are no bond-valence curves available for Fe^{2+}-Cl bonds. However, we can estimate the relative strengths of the interactions by simple geometrical arguments. When O3 = OH^- or F^-, O3 receives ~1 vu from 2M1 + M3 cations, the case for crystal Cl(0). However, in samples Cl(1) and Cl(2), the M1-O1, M1-O2, and M3-O1 bonds do not lengthen with the substitution of Fe^{2+} for Mg, and these bonds must therefore become stronger. That requires a weakening of the bonds to O3', which thus receives <1 vu from its coordinating 2M1 + M3 cations.

A sites

As discussed above, Cl at O3' receives <1 vu from the cations of the octahedral strip. It therefore must bond to another cation; the only possibility is the alkali cation in the A cavity, which can occupy the three A, Am, and A2 positions (Oberti et al., 1992). The geometry of the A cavity and the distances between cations A, Am, and A2 and anions O3 and O3' are given in Table 3. It is immediately apparent that the O3' site is much closer to the alkali cation than the O3 site. In particular, the very short Am-O3' distance (2.86–2.93 Å) observed in Cl-bearing amphiboles implies a strong bond interaction. Also the A-O3' distance (3.30 Å) and A2-O3' distance (3.36–3.37 Å) are in the range of typical K-Cl distances in inorganic compounds [cf. [6]3.15–3.27 in $K_2SnCl_4 \cdot H_2O$; [12]3.44 in K_2PtCl_6; [12]3.46–3.57 Å in $K_2PbCl_2(NO_2)_4$]. A Na-Cl interaction is also feasible (cf. [6]2.82 Å in NaCl), but the A-O3' and A2-O3' distances, combined with the observed site preference of K for Am, are in favor of K as the bonding A cation.

THE INCORPORATION OF Cl INTO THE AMPHIBOLE STRUCTURE

There are two ideal models by which the amphibole structure can accommodate Cl^- replacing OH^- at O3: (1) the octahedral strip could maintain its normal dimensions, and the Cl^- anion would occupy a hole that is too small and project into the A cavity; (2) the octahedral strip could expand such that the large Cl^- anion could be more or less coplanar with the other anions of the strip.

It is apparent from the split nature of the O3 site and the larger x parameter of O3' relative to O3 (0.16 vs. 0.11) that model 1 is at least partly operative. However, inspection of the M1-M1 distances (Table 3) shows that the octahedral strip also expands in response to substitution of Cl^- for OH^-. The increase in M1-M1 separation from crystal Cl(0) to crystal Cl(2) is far greater than what can be ascribed to the increase in Fe^{2+} content of the octahedral strip and must be due to the occurrence of Cl^- as the monovalent anion. However, the increase in M1-M1 across the series (~0.20 Å) is less than the displacement of the Cl^- at O3' relative to OH^- at O3 (~0.56 Å), indicating that model 1 is the more important of the two mechanisms.

VARIATION IN UNIT-CELL DIMENSIONS WITH $Cl^- \rightleftharpoons OH^-$ SUBSTITUTION

The effects of the $Cl^- \rightleftharpoons OH^-$ substitution on amphibole cell dimensions are most clearly seen by comparing samples Cl(0) and Cl(2) [comparison with Cl(1) is complicated by different [4]Al and [6]Fe^{3+} contents]. Not surprisingly, there is a significant increase in cell volume (Table 1) with increasing Cl. However, the behavior of the individual cell dimensions is distinctly anisotropic, with expansions of 2.7, 5.5, and 5.3%, respectively, for a, b, and c. This is very interesting, as we have seen above that the principal mechanism for the incorporation of Cl^- involves anion displacement along [100], rather than expansion of the octahedral strip in the (011) plane. This means that, although the Cl^- is displaced along [100] into the A cavity, the A cavity does not expand along [100]. Of course, that is in line with the bonding interaction between Cl^- and K observed at the A site; Cl comes closer to the A cation, and hence the cavity does not expand to any great extent.

COMPOSITIONAL IMPLICATIONS OF THE Cl INCORPORATION MECHANISMS

The A-O3 interaction

As indicated above, there is a bonding interaction between Cl^- and the A cation, especially involving the Am position. The A cavity is very large, and the A-O3 distance is large, even in Cl-bearing amphiboles in which Cl^- projects out of the octahedral strip into the A cavity (Fig. 2). Hence this bonding interaction is greatly pro-

moted by the occurrence of K as the A cation and because K preferentially orders at the closer Am position. Hence one expects a strong correlation between K and Cl contents in amphibole structures, and this has been observed frequently in the past (e.g., Suwa et al., 1987; Castelli, 1988; Enami et al., 1993).

The M1,3-O3,3′ interactions

As indicated above, the variation in M1-O3, M3-O3, M1-O3′, and M3-O3′ distances across the series suggests local ordering of Fe^{2+} and Cl^-. This indicates that the structure strongly prefers Fe^{2+}-Cl pairs to Mg-Cl pairs, accounting for the strong correlation between Fe^{2+} and Cl contents observed in previous work (Mevel, 1984; Volfinger et al., 1985; Gulyaeva et al., 1986; Suwa et al., 1987; Castelli, 1988; Enami et al., 1993). It should be noted here that this short-range order is not a geometrical effect, but a local chemical effect, dictated by the preference of Cl for $Cl-Fe^{2+}$ rather than Cl-Mg bonds.

Interactions between the octahedral strip and tetrahedral chain

As Cl content increases, so does that of Fe^{2+}, and that has the effect of considerably increasing the dimensions of the octahedral strip. That being the case, the tetrahedral chain has to expand to remain linked to the octahedral strip. This expansion may occur in two ways: (1) straightening of the chain, as measured by the O5-O6-O5 angle; (2) substitution of [4]Al for Si, which increases the size of the tetrahedra. Inspection of Table 3 shows that there is significant straightening of the chain [164.5 → 168.7° from crystal Cl(0) to Cl(2)]. However, the chain cannot straighten any farther and maintain the necessary coordination about the M4 site (cf. Hawthorne, 1983, Fig. 18). Consequently, there must be significant substitution of [4]Al for Si. In line with this argument, correlations of [4]Al with Cl have been noted by Mevel (1984), Vanko (1986), Suwa et al. (1987), Castelli (1988), Morrison (1991), and Enami et al. (1993).

REFERENCES CITED

Bellanca, A. (1948) The structure of erythrosiderite. Periodico di Mineralogia—Roma, 17, 59–67.
Borley, G.D. (1962) Amphiboles from the younger granites of Nigeria. I. Chemical classification. Mineralogical Magazine, 33, 358–376.
Buddington, A.F., and Leonard, B.F. (1953) Chemical petrology and mineralogy of hornblendes in northwest Adirondack granitic rocks. American Mineralogist, 38, 891–902.
Castelli, D. (1988) Chlorpotassium ferro-pargasite from Sesia-Lanzo marbles (Western Italian Alps): A record of highly saline fluids. Rendiconti della Società Italiana di Mineralogia e Petrologia, 43, 129–138.

Dick, L.A., and Robinson, G.W. (1979) Chlorine-bearing potassian hastingsite from a sphalerite skarn in southern Yukon. Canadian Mineralogist, 17, 25–26.
Enami, M., Liou, J.G., and Bird, D.K. (1993) Cl-amphibole in the Salton Sea geothermal system, California. Canadian Mineralogist, 30, in press.
Gulyaeva, T.Ya., Gorelikova, N.V., and Karabtsov, A.A. (1986) High potassium-chlorine-bearing hastingsites in skarns from Primorye, far east USSR. Mineralogical Magazine, 50, 724–728.
Hawthorne, F.C. (1983) The crystal chemistry of the amphiboles. Canadian Mineralogist, 21, 173–480.
Ito, E., and Anderson, A.T., Jr. (1983) Submarine metamorphism of gabbros from the Mid-Cayman Rise: Petrographic and mineralogical constraints on hydrothermal processes at slow-spreading ridges. Contributions to Mineralogy and Petrology, 82, 371–388.
Kaminemi, D.C., Bonardi, M., and Rao, A.T. (1982) Halogen-bearing minerals from Airport Hill, Visakhapatnam, India. American Mineralogist, 67, 1001–1004.
Krutov, G.A. (1936) Dashkessanite: A new chlorine amphibole of the hastingsite group. Døklady Akademie Nauk SSSR (Geological Series), 341–373.
Leelanadam, C. (1970) Chemical mineralogy of hornblendes and biotites from the charnockitic rocks of Kondapalli, India. Journal of Petrology, 11, 475–505.
Lehman, M.S., and Larsen, F.K. (1974) A method for location of the peaks in step-scan-measured Bragg reflections. Acta Crystallographica, A30, 580–586.
Mevel, C. (1984) Le métamorphisme dans la croûte océanique. Ph.D. thesis, Université Pierre et Marie Curie, Paris, France.
Morrison, J. (1991) Compositional constraints on the incorporation of Cl into amphiboles. American Mineralogist, 76, 1920–1930.
North, A.C.T., Phillips, D.C., and Mathews, F.S. (1968) A semi-empirical method of absorption correction. Acta Crystallographica, A24, 351–359.
Oberti, R., Ungaretti, L., Cannillo, E., and Hawthorne, F.C. (1992) The behaviour of Ti in amphiboles. I. Four- and six-coordinated Ti in richterite. European Journal of Mineralogy, 4, 425–439.
Penfold, B.R., and Grigor, J.A. (1959) The crystal structure of iron (II) chloride tetrahydrate. Acta Crystallographica, 12, 850–856.
Pouchou, J.L., and Pichoir, F. (1984) A new model for quantitative analysis. I. Application to the analysis of homogenous samples. La recherche Aérospatiale, 5, 47–65.
———(1985) 'PAP' $\phi(\rho Z)$ procedure for improved quantitative microanalysis. Microbeam Analysis, 104–106.
Suwa, K., Enami, M., and Horiuchi, T. (1987) Chlorine-rich potassium hastingsite from West Ongul Island, Lützow-Holm Bay, East Antarctica. Mineralogical Magazine, 51, 709–714.
Ungaretti, L. (1980) Recent developments in X-ray single crystal diffractometry applied to the crystal-chemical study of amphiboles. Godišnjak Jugoslavenskog centra za Kristalografiju, 15, 29–65.
Ungaretti, L., Smith, D.C., and Rossi, G. (1981) Crystal-chemistry by X-ray structure refinement and electron microprobe analysis of a series of sodic-calcic to alkali amphiboles from the Nybö eclogite pod. Bulletin de Minéralogie, 104, 100–112.
Ungaretti, L., Lombardo, L., Domeneghetti, C., Rossi, G. (1983) Crystal-chemical evolution of amphiboles from eclogitised rocks of the Sesia Lanzo Zone, Italian Western Alps. Bulletin de Minéralogie, 106, 645–672.
Vanko, D.A. (1986) High-chlorine amphiboles from oceanic rocks: Product of highly saline hydrothermal fluids. American Mineralogist, 71, 51–59.
Volfinger, M., Robert, J.-L., Vielzeuf, D., and Neiva, A.M.R. (1985) Structural control of the chlorine content of OH-bearing silicates (micas and amphiboles). Geochimica et Cosmochimica Acta, 49, 37–48.